Optimal design of feedback coils for the control of external modes in tokamaks

R. Fitzpatrick and E. P. Yu

Citation: Physics of Plasmas (1994-present) **5**, 2340 (1998); doi: 10.1063/1.872908
View online: http://dx.doi.org/10.1063/1.872908
View Table of Contents: http://scitation.aip.org/content/aip/journal/pop/5/6?ver=pdfcov
Published by the AIP Publishing

Optimal design of feedback coils for the control of external modes in tokamaks

R. Fitzpatrick and E. P. Yu
Institute for Fusion Studies, Department of Physics, The University of Texas at Austin, Austin, Texas 78712

(Received 27 October 1997; accepted 4 March 1998)

A formalism is developed for optimizing the design of feedback coils placed around a tokamak plasma in order to control the resistive shell mode. It is found that feedback schemes for controlling the resistive shell mode fail whenever the distortion of the mode structure by the currents circulating in the feedback coils becomes too strong, in which case the mode escapes through the gaps between the coils, or through the centers of the coils. The main aim of the optimization process is to reduce this distortion by minimizing the coupling of different Fourier harmonics due to the feedback currents. It is possible to define a quantity α_0 which parametrizes the strength of the coupling. Feedback fails for $\alpha_0 \geq 1$. The optimization procedure consists of minimizing α_0 subject to practical constraints. If there are very many evenly spaced feedback coils surrounding the plasma in the poloidal direction then the optimization can be performed analytically. Otherwise, the optimization must be performed numerically. The optimal configuration is to have many, large, overlapping coils in the poloidal direction. © *1998 American Institute of Physics.* [S1070-664X(98)01706-6]

I. INTRODUCTION

Pressure gradient driven external kink modes often limit the maximum achievable β in tokamak plasmas.[1] Since fusion reactivity scales roughly like β^2, a practical method of improving the stability of external kink modes would clearly be of very great benefit to the magnetic fusion program. Actually, it is well known that external kink modes become much more stable in tokamaks when the plasma is surrounded by a close fitting, perfectly conducting shell.[2] Unfortunately, such a scheme is quite impractical: all realizable conducting shells in reactor relevant tokamak experiments possess non-negligible resistivity. When a tokamak plasma is surrounded by a close fitting, resistive shell, the relatively fast growing external kink mode is converted into the far more slowly growing ''resistive shell mode.'' The latter mode grows on the characteristic L/R time of the shell, and generally has virtually identical stability boundaries to those of the external kink mode in the absence of a conducting shell.[3] (Rapid plasma rotation can have a stabilizing effect on the resistive shell mode, relative to the free boundary external kink mode,[4–6] but this effect is expected to be negligibly small in a reactor-sized plasma, and is, therefore, neglected in this paper.) The L/R time of a conventional resistive shell is long compared to most plasma time scales, but is still generally much shorter than the duration of a tokamak discharge. Thus it is necessary to stabilize the resistive shell mode, as well as the external kink mode, in order to have any chance of raising the limiting β of a tokamak plasma using an external conducting shell.

Consider a large aspect-ratio, low-β, circular cross-section tokamak plasma surrounded by a thin, uniform, resistive shell.[7] (In low-β tokamaks, external kink modes are driven unstable by current gradients, rather than by pressure gradients. However, the interaction of a current gradient driven external kink mode with an external conducting shell is essentially the same as that of a pressure gradient driven mode. This paper, therefore, concentrates on current driven external kink modes, since these are far easier to treat analytically than pressure driven modes.) The plasma and shell are approximated as a cylinder of radius a, and a concentric cylindrical shell of radius $r_w > a$, respectively. Consider a simply connected circuit C which lies entirely within the shell. Let S be the surface which spans C, and also lies entirely within the shell. The sense of circulation around C is assumed to be such that the normal to S points radially outwards. The perturbed circuit equation for C takes the form

$$K_C = -\gamma \tau_w \Phi_C, \tag{1}$$

where

$$K_C = r_w \oint_C \mu_0 \delta \mathbf{I} \cdot d\mathbf{l} \tag{2}$$

is (proportional to) the line integral of the radially integrated perturbed eddy current density $\delta \mathbf{I}(\theta, z)$ around C, and

$$\Phi_C = \int_S \delta \mathbf{B} \cdot \hat{\mathbf{r}} dS \tag{3}$$

is the perturbed magnetic flux linking C. Here (r, θ, z) are standard right-handed cylindrical polar coordinates, $\delta \mathbf{B}$ is the perturbed magnetic field, and

$$\tau_w = \mu_0 \sigma_w \delta_w r_w \tag{4}$$

is the L/R time, or ''time constant,'' of the shell. The quantities δ_w and σ_w are the shell thickness and conductivity, respectively. Finally, γ is the growth rate of the resistive shell mode.

Note that all of the analysis in this paper is performed in the ''thin shell'' limit, in which the skin depth of the perturbed magnetic field in the shell material is much greater than the thickness of the shell, but much less than its radius.

In this limit, there is negligible radial variation of the perturbed magnetic field and the perturbed eddy current density across the shell. The thin shell limit is valid whenever

$$\frac{\delta_w}{r_w} \ll |\gamma| \tau_w \ll \frac{r_w}{\delta_w}. \tag{5}$$

It is reasonable to adopt this limit provided that the thickness of the shell is much less than its minor radius, as is assumed to be the case, and also that the analysis is restricted to those cases in which the external kink mode is unstable in the absence of a conducting shell, but would become completely stable were the resistive shell replaced by a perfectly conducting shell.

Equation (1), which is valid for all circuits C which lie within the shell, completely specifies the physics of the shell. For an m,n resistive shell mode, the physics of the plasma and the vacuum region surrounding the shell can be summed up in a single relation,

$$K_C = -\Delta_w^{m,n} \Phi_C, \tag{6}$$

which is also valid for every circuit C lying within the shell. The parameter $\Delta_w^{m,n}$ is called the ''shell stability index'' for the m,n mode, and can be uniquely determined from the linearized equations of marginally stable ideal magnetohydrodynamics (MHD) in the region outside the shell. Equations (1) and (6) yield the dispersion relation for the m,n resistive shell mode,

$$\gamma \tau_w = \Delta_w^{m,n}. \tag{7}$$

According to this dispersion relation, if the shell stability index $\Delta_w^{m,n}$ is positive then the mode grows (without rotation in the laboratory frame) on the L/R time of the shell. However, if $\Delta_w^{m,n}$ is negative then the mode is stable.

Consider a general circuit C lying within the shell. Suppose that a thin feedback coil, running along the path of C, is installed just outside the shell. The feedback coil is accompanied by a high resistance detector loop which measures the perturbed magnetic flux Φ_C linking the coil. Let the feedback controlled current driven around the coil be proportional to minus the flux linking the coil. The feedback modified circuit equation for C then takes the form

$$K_C = -(\gamma \tau_w + \Delta_w^{m,n} Q) \Phi_C, \tag{8}$$

where Q is the ''gain'' in the feedback circuit. Suppose that every circuit contained within the shell is modified by feedback in the manner described above. It follows that every circuit is governed by Eq. (8). Equations (6) and (8) can then be combined to give the feedback modified dispersion relation for the m,n resistive shell mode:

$$\gamma \tau_w = \Delta_w^{m,n} (1 - Q). \tag{9}$$

In the absence of feedback (i.e., $Q=0$), all of the eddy currents which are required to flow in the shell by the ''outer solution'' (i.e., the linearized equations of marginally stable ideal MHD in the region outside the shell) are generated by magnetic induction inside the shell, entailing the growth of the mode (assuming that $\Delta_w^{m,n} > 0$). As the gain, Q, in the feedback circuits is gradually increased from zero, an increasing fraction of the required eddy currents is supplied by the feedback coils, and less current is generated by induction, so the growth rate of the mode is reduced. Eventually, when $Q=1$, all of the required eddy currents are supplied by the feedback coils, and there is no need for any inductive current, so the mode does not grow. For $Q>1$, the feedback coils supply too much eddy current, and a negative inductive current is generated in the shell, which causes the mode to decay.

Of course, the feedback scheme outlined above is completely impractical, since it would require an infinite number of feedback coils: one for every possible circuit in the shell. In a practical feedback system, which employs a finite number of coils, only a small fraction of the circuits contained within the shell can be modified by feedback. In other words, only a select few circuits are governed by Eq. (8), the remainder are governed by Eq. (1). It seems likely, therefore, that a practical feedback scheme is going to be far less effective than the ideal scheme outlined above. The main question addressed in this paper is as follows. How is it possible to optimize the design of the feedback coils, subject to certain practical constraints (e.g., only a fixed number of coils, or only a certain fraction of the shell covered by coils), such that the feedback scheme approaches as closely as possible to the ideal feedback scheme described above?

II. PRELIMINARY ANALYSIS

A. Introduction

Standard cylindrical coordinates (r,θ,z) are adopted. The plasma is approximated as a cylinder of radius a. The system is assumed to be periodic in the z direction, with periodicity length $2\pi R_0$, where R_0 is the simulated major radius of the plasma. It is convenient to define a simulated toroidal angle $\phi = z/R_0$.

B. Basic definitions

The perturbed magnetic field is written

$$\delta \mathbf{B} = \nabla \psi \wedge \hat{\mathbf{z}}, \tag{10}$$

where $\psi(r,\theta,\phi)$ is the perturbed poloidal magnetic flux. The magnetic field can only be written in this form provided that

$$\left| \frac{1}{r} \frac{\partial \psi}{\partial \theta} \right| \gg \left| \frac{1}{R_0} \frac{\partial \psi}{\partial \phi} \right|. \tag{11}$$

Fourier transformation of the perturbed poloidal flux yields

$$\psi(r,\theta,\phi) = \sum_m \Psi^m(r) \exp[i(m\theta - n\phi)]. \tag{12}$$

All perturbed quantities are assumed to possess a common toroidal mode number, n. In the large aspect-ratio tokamak limit, characterized by [see Eq. (11)]

$$|m| \gg |n| \epsilon_w, \tag{13}$$

where $\epsilon_w = r_w/R_0 \ll 1$, the linearized equations of marginally stable ideal MHD reduce to[2]

$$\frac{1}{r}\frac{d}{dr}\left(r\,\frac{d\Psi^m}{dr}\right)-\frac{m^2}{r^2}\,\Psi^m+\frac{\mu_0 J_\phi'}{B_\theta(nq/m-1)}\,\Psi^m=0. \quad (14)$$

Here $\mathbf{B}=[0,B_\theta(r),B_\phi]$ is the equilibrium magnetic field, $q(r)=rB_\phi/R_0B_\theta$ is the ''safety factor,'' and $J_\phi'\equiv dJ_\phi/dr$ is the radial derivative of the equilibrium ''toroidal'' plasma current, $\mu_0 J_\phi(r)=(1/r)d(rB_\theta)/dr$.

C. Shell physics

Suppose that the plasma is surrounded by a thin, rigid, concentric, conducting shell. In the thin shell limit, it is possible to unambiguously define a ''shell flux''

$$\Psi_w(\theta,\phi)\equiv\psi(r_w,\theta,\phi), \quad (15)$$

where r_w is the minor radius of the shell. Note that even though ψ is continuous across the shell, in general, its radial derivative is discontinuous.

In the thin shell limit, the eddy currents induced in the shell have no significant radial variation. Hence the radially integrated perturbed eddy current density can be written

$$\mu_0\,\delta\mathbf{I}_w=\nabla J_w\wedge\hat{\mathbf{r}}, \quad (16)$$

where $J_w(\theta,\phi)$ is the eddy current stream function. It is helpful to define the quantity

$$\Delta\Psi_w(\theta,\phi)=\left[r\,\frac{\partial\psi(r,\theta,\phi)}{\partial r}\right]_{r_{w-}}^{r_{w+}}, \quad (17)$$

which parametrizes the jump in the radial derivative of ψ across the shell.

Ampère's law radially integrated across the shell yields

$$\Delta\Psi_w=\frac{\partial J_w}{\partial\theta} \quad (18)$$

in the large aspect-ratio limit. Ohm's law combined with Faraday's law gives

$$\gamma\tau_w\,\frac{\partial\Psi_w}{\partial\theta}=r_w^2\nabla^2 J_w, \quad (19)$$

where the shell time constant, τ_w, is defined in Eq. (4).

It is helpful to Fourier transform the shell flux $\Psi_w(\theta,\phi)$ and the function $\Delta\Psi_w(\theta,\phi)$:

$$\Psi_w(\theta,\phi)=\sum_m \Psi_w^m\,\exp[i(m\theta-n\phi)], \quad (20a)$$

$$\Delta\Psi_w(\theta,\phi)=\sum_m \Delta\Psi_w^m\,\exp[i(m\theta-n\phi)]. \quad (20b)$$

Equations (18) and (19) yield

$$\Delta\Psi_w^m=imJ_w^m, \quad (21)$$

and

$$\gamma\tau_w\Psi_w^m=imJ_w^m, \quad (22)$$

respectively, in the large aspect-ratio limit.

D. Asymptotic matching

Equation (14) governs the structure of the resistive shell mode in the ''outer region'' (i.e., everywhere apart from inside the shell). This equation is manifestly singular at any ''rational flux surface,'' for which $q=m/n$, except when such surfaces are situated in the vacuum region outside the plasma (where $J_\phi=0$). A physically acceptable solution of Eq. (14) must satisfy physical boundary conditions at $r=0$ and $r=\infty$, with Ψ^m continuous across the shell. In addition, Ψ^m must be zero at any rational surface lying inside the plasma. The latter constraint comes about because modes which interact strongly with the shell tend to rotate very slowly in the laboratory frame, and, therefore, do not reconnect magnetic flux inside the plasma, which is usually rotating substantially faster than the rate of resistive reconnection.[8] In general, there is a discontinuity in the radial derivative of Ψ^m at $r=r_w$. The shell stability index

$$\Delta_w^m=\left[r\,\frac{d\Psi^m}{dr}\Big/\,\Psi^m\right]_{r_{w-}}^{r_{w+}} \quad (23)$$

is uniquely defined for every poloidal harmonic, except for the $m=0$ harmonic. The $m=0$ harmonic is a special case because the inequality (13) is not satisfied for this poloidal harmonic, so the usual large aspect-ratio tokamak approximations break down. Note that the quantity Δ_w^m is equivalent to the quantity $\Delta_w^{m,n}$, defined in Sec. I: the superscript n is redundant, since all perturbed quantities are assumed to possess a common toroidal mode number, n.

Asymptotic matching between the ''inner region'' (i.e., the shell) and the ''outer region'' yields

$$\Delta\Psi_w^m=\Delta_w^m\Psi_w^m. \quad (24)$$

Equations (21), (22), and (24) reduce to the standard dispersion relation for the m,n resistive shell mode:

$$\gamma\tau_w=\Delta_w^m. \quad (25)$$

E. The resistive shell mode

In general, for physically plausible plasma current profiles, at most one of the Δ_w^m is positive at any given time.[9] Suppose that $\Delta_w^{m_0}>0$, with $\Delta_w^m<0$ for all $m\neq m_0$. Here the m_0,n harmonic is termed the ''central harmonic.'' It follows that the m_0,n resistive shell mode is unstable, with growth rate

$$\gamma\tau_w=\Delta_w^{m_0}, \quad (26)$$

and that all other resistive shell modes are stable.

Now, the solution of Eq. (14) in the vacuum region outside the plasma consists of a linear combination of $r^{+|m|}$ and $r^{-|m|}$ functions. It easily follows that $\Delta_w^{m_0}$ can be written in the form

$$\Delta_w^{m_0}=\frac{2m_0}{(r_c/r_w)^{2m_0}-1}, \quad (27)$$

assuming that $m_0>0$. The quantity r_c is termed the ''critical radius.'' According to Eqs. (26) and (27), the growth rate of the resistive shell mode asymptotes to infinity as $r_w\to r_c$. In

fact, $r_w = r_c$ corresponds to the ideal stability boundary. For $r_w > r_c$, the m_0, n ideal external kink mode becomes unstable, and grows on some extremely short time scale determined by plasma inertia. In the following, it is assumed that $r_w < r_c$, so that the only unstable mode is the m_0, n resistive shell mode.

For sideband harmonics (i.e., $m \neq m_0$), it is usually a good approximation to write

$$\Delta_w^m \simeq -2|m|. \tag{28}$$

In the limit $|m| \gg 1$, this approximation becomes exact.

III. THE FEEDBACK MODIFIED DISPERSION RELATION

A. Introduction

Suppose that a set of feedback coils is installed immediately outside the shell. The radially integrated current density carried by the feedback coils is written

$$\mu_0 \delta \mathbf{I}_f = \nabla J_f \wedge \hat{\mathbf{r}}, \tag{29}$$

where $J_f(\theta, \phi)$ is the feedback current stream function. Equations (22) and (24) remain valid, so

$$\gamma \tau_w \Psi_w^m = i m J_w^m, \tag{30a}$$

$$\Delta \Psi_w^m = \Delta_w^m \Psi_w^m, \tag{30b}$$

but Eq. (21) generalizes to

$$\Delta \Psi_w^m = i m (J_w^m + J_f^m). \tag{31}$$

Equations (30) and (31) yield

$$i m J_f^m = (\Delta_w^m - \gamma \tau_w) \Psi_w^m. \tag{32}$$

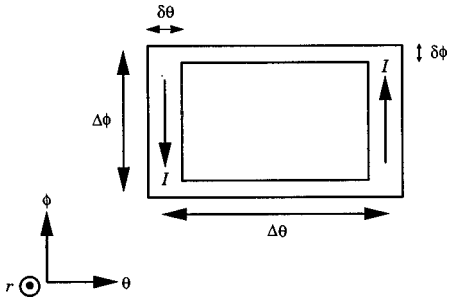

FIG. 1. An individual feedback coil.

B. The feedback coils

The distribution of feedback coils is assumed to be toroidally symmetric. It is further assumed that there are sufficient, closely spaced coils in the toroidal direction and that there is negligible coupling of different toroidal harmonics by the feedback currents.

Suppose, for the sake of simplicity, that all of the feedback loops are identical, and consist of thin, rectangular, saddle coils, as illustrated in Fig. 1. The poloidal and toroidal angular extents of each coil are $\Delta\theta$ and $\Delta\phi$, respectively. Furthermore, the angular widths of the toroidal and poloidal legs of each coil are $\delta\theta$ and $\delta\phi$, respectively. Suppose that there are M coils in the poloidal direction, with the kth coil centered on poloidal angle θ_k.

Let I_k be the total current circulating around the kth coil. For the sake of simplicity, this current is assumed to be uniformly distributed throughout the coil. It follows from Eq. (29) that

$$\frac{\partial J_f}{\partial \theta} = \begin{cases} -\mu_0 I_k / \delta\theta & \text{for } \theta_k + \Delta\theta/2 - \delta\theta/2 < \theta < \theta_k + \Delta\theta/2 + \delta\theta/2 \\ +\mu_0 I_k / \delta\theta & \text{for } \theta_k - \Delta\theta/2 - \delta\theta/2 < \theta < \theta_k - \Delta\theta/2 + \delta\theta/2 \\ 0 \quad \text{otherwise} & \end{cases}, \tag{33}$$

in the large aspect-ratio limit, where k runs from 1 to M. Now,

$$J_f^m = \oint \frac{\partial J_f}{\partial \theta} \frac{e^{-im\theta}}{im} \frac{d\theta}{2\pi}, \tag{34}$$

giving

$$J_f^m = \frac{2\mu_0}{\pi \delta\theta} \frac{\sin(m\delta\theta/2)\sin(m\Delta\theta/2)}{m^2} \sum_{k=1,M} I_k e^{-im\theta_k}. \tag{35}$$

Note that the common $e^{-in\phi}$ dependence of perturbed quantities has been neglected for ease of notation.

C. The feedback algorithm

Suppose that the kth feedback coil is accompanied by a detector loop, of equal area, which measures the perturbed magnetic flux

$$\Phi_k = \int_{k\text{th coil}} \delta \mathbf{B} \cdot \hat{\mathbf{r}} \, dA = R_0 \Delta\phi \{\Psi_w(\theta_k + \Delta\theta/2) - \Psi_w(\theta_k - \Delta\theta/2)\} \tag{36}$$

passing through the coil. It is easily demonstrated that

$$\Phi_k = 2 i R_0 \Delta\phi \sum_m \sin(m\Delta\theta/2) \Psi_w^m e^{im\theta_k}. \tag{37}$$

The feedback algorithm adopted in this paper is very straightforward: the current driven through each feedback coil is directly proportional to minus the perturbed magnetic flux linking the coil. It follows that

$$\mu_0 I_k = -\left(\frac{\Delta_w^{m_0} \delta\theta}{2 R_0 \Delta\phi} \right) Q \Phi_k, \tag{38}$$

where Q is the ''gain'' in the feedback circuits. Note that this definition of the gain is entirely consistent with that employed in Sec. I.

D. The dispersion relation

Equations (32), (35), (37), and (38) can be combined to give the infinite dimensional matrix eigenvalue equation

$$(\mathbf{G}-\lambda\mathbf{I})\boldsymbol{\Psi}_w=\mathbf{0}, \tag{39}$$

where $\lambda=\gamma\tau_w$, $\boldsymbol{\Psi}_w$ is the vector of the Ψ_w^m values, $\mathbf{I}$ is the unit matrix, $\mathbf{0}$ is the zero vector, and

$$G^{mm'}=\Delta_w^m\delta^{mm'}-\Delta_w^{m_0}L^{mm'}. \tag{40}$$

Here

$$L^{mm'}=\hat{Q}\,\frac{m_0}{m}\,\frac{\sin(m\,\delta\theta/2)\sin(m\Delta\,\theta/2)\sin(m'\Delta\,\theta/2)}{\sin(m_0\delta\theta/2)\sin^2(m_0\Delta\,\theta/2)} \times\sum_{k=1,M}\frac{e^{i(m'-m)\theta_k}}{M}, \tag{41}$$

where

$$\hat{Q}=\frac{Q}{Q_0} \tag{42}$$

and

$$Q_0=\frac{\pi}{2}\,\frac{m_0}{M}\,\frac{1}{\sin(m_0\delta\theta/2)\sin^2(m_0\Delta\,\theta/2)}. \tag{43}$$

Note that there is no coupling to the $m=0$ harmonic, since $L^{0m'}=L^{m0}=0$ for all nonzero values of m and m'.

Equation (39) can be solved using standard methods. The physical eigenvalue of the **G** matrix gives the feedback modified growth rate of the resistive shell mode. The corresponding eigenvector gives the Fourier harmonics of the shell flux. It is possible to reconstruct the currents I_k circulating around the feedback coils using this information. However, it is generally simpler to solve directly for the coil currents, as described below.

Equations (32), (35), (37), and (38) can also be combined to give the square, M-dimensional, homogeneous matrix equation

$$\mathbf{A}\hat{\mathbf{I}}=\mathbf{0}, \tag{44}$$

where $\hat{\mathbf{I}}$ is the vector of the

$$\hat{I}_k=I_k e^{-im_0\theta_k} \tag{45}$$

values, and

$$A_{kk'}=\delta_{kk'}-B_{kk'}. \tag{46}$$

Here

$$B_{kk'}=\frac{\hat{Q}}{M}\sum_m^{m\neq 0}\frac{\Delta_w^{m_0}}{\Delta_w^m-\gamma\tau_w}\,\frac{m_0}{m}\,\frac{\sin(m\,\delta\theta/2)\sin^2(m\Delta\,\theta/2)}{\sin(m_0\delta\theta/2)\sin^2(m_0\Delta\,\theta/2)} \times e^{i(m-m_0)(\theta_k-\theta_{k'})}. \tag{47}$$

The dispersion relation can be expressed as a polynomial in the feedback modified growth rate γ of the resistive shell mode by setting the determinant of the **A** matrix equal to zero. The eigenvector of the **A** matrix, corresponding to the eigenvalue zero, specifies the currents circulating around the feedback coils.

IV. EVENLY SPACED COILS

A. Introduction

Suppose that the feedback coils are evenly spaced, so that

$$\theta_k=(k-1)\,\frac{2\pi}{M} \tag{48}$$

for $k=1,M$. It follows that

$$\frac{1}{M}\sum_{k=1,M}e^{i(m'-m)\theta_k}=\begin{cases}1 & \text{if } m'=m+jM\\ 0 & \text{otherwise}\end{cases}, \tag{49}$$

where j is an integer. Thus from Eq. (41),

$$L^{mm'}=\hat{Q}\begin{cases}\dfrac{m_0}{m}\,\dfrac{\sin(m\,\delta\theta/2)\sin(m\Delta\,\theta/2)\sin(m'\Delta\,\theta/2)}{\sin(m_0\delta\theta/2)\sin^2(m_0\Delta\,\theta/2)} & \text{if } m'=m+jM\\ 0 & \text{otherwise}\end{cases}. \tag{50}$$

It is clear from Eqs. (39), (40), and (50) that only the

$$m=m_0+jM \tag{51}$$

poloidal harmonics need be included in the calculation of the feedback modified growth rate of the intrinsically unstable m_0,n resistive shell mode.

B. The dispersion relation

Retaining only the poloidal harmonics specified above, the **A** matrix reduces to

$$\mathbf{A}=\mathbf{I}-B\mathbf{1}, \tag{52}$$

where **1** is an M-dimensional square matrix whose elements are all unity, and

$$B=\frac{\hat{Q}}{M}\sum_{j,m\neq 0}^{m=m_0+jM}\frac{\Delta_w^{m_0}}{\Delta_w^m-\gamma\tau_w}\,\frac{m_0}{m}\,\frac{\sin(m\,\delta\theta/2)\sin^2(m\Delta\,\theta/2)}{\sin(m_0\delta\theta/2)\sin^2(m_0\Delta\,\theta/2)}. \tag{53}$$

Here use has been made of Eqs. (46) and (47). The solution of the homogeneous matrix equation (44), with the **A** matrix given by Eq. (52), is

$$\hat{I}_k = \hat{I}, \tag{54a}$$

$$B = 1/M, \tag{54b}$$

where $\hat{I}$ is a constant. Thus the currents circulating around the feedback coils are given by

$$\hat{I}_k = \hat{I} e^{\,i m_0 \theta_k}, \tag{55}$$

and the feedback modified dispersion relation of the m_0, n resistive shell mode takes the form

$$1 = \hat{Q} \sum_{j,m\neq 0}^{m=m_0+jM} \frac{\Delta_w^{m_0}}{\Delta_w^m - \gamma\tau_w} \frac{m_0}{m} \frac{\sin(m\delta\theta/2)\sin^2(m\Delta\theta/2)}{\sin(m_0\delta\theta/2)\sin^2(m_0\Delta\theta/2)}. \tag{56}$$

C. Approximate solution of the dispersion relation: I

The dispersion relation (56) can be written

$$1 = \hat{Q}\left(\frac{\Delta_w^{m_0}}{\Delta_w^{m_0} - \gamma\tau_w} - \alpha\right), \tag{57}$$

where

$$\alpha = \sum_{j,j\neq 0,m\neq 0}^{m=m_0+jM} \frac{\Delta_w^{m_0}}{\gamma\tau_w - \Delta_w^m} \frac{m_0}{m} \frac{\sin(m\delta\theta/2)\sin^2(m\Delta\theta/2)}{\sin(m_0\delta\theta/2)\sin^2(m_0\Delta\theta/2)}. \tag{58}$$

parametrizes the strength of the coupling between the intrinsically unstable m_0, n harmonic and the various sideband harmonics (i.e., those m, n harmonics for which $m \neq m_0$). This coupling takes place because the currents which circulate around the feedback coils do not possess pure m_0, n helical symmetry.

Suppose that the coupling to the sideband harmonics is negligible (i.e., $\alpha = 0$). This is likely to be the case when the m_0, n resistive shell mode lies close to marginal stability (i.e., when $\Delta_w^{m_0}$ is small and positive). In the absence of sideband coupling, Eq. (57) can be rearranged to give[10]

$$\gamma\tau_w = \Delta_w^{m_0}(1 - Q/Q_0), \tag{59}$$

where use has been made of Eq. (42). This dispersion relation is of the same form as the dispersion relation (9) obtained for the idealized feedback scheme discussed in Sec. I, except that in the idealized scheme the critical value of the gain beyond which the mode is stabilized is $Q = 1$, whereas in the present scheme the critical value of the gain is $Q = Q_0$. Recall, from Eq. (43), that

$$Q_0 = \frac{\pi}{M\delta\theta} \frac{1}{\sin^2(m_0\Delta\theta/2)}. \tag{60}$$

Here it is assumed that $m_0\delta\theta \ll 1$, as seems reasonable.

Two conditions must be satisfied in order for the present feedback scheme (in the absence of mode coupling) to become as efficient as the idealized scheme discussed in Sec. I. First, the poloidal extent of each feedback coil must equal half the poloidal wavelength of the intrinsically unstable m_0, n harmonic. In other words,

$$\Delta\theta = \frac{\pi}{m_0}. \tag{61}$$

Second, a sufficiently large number of feedback coils must be placed around the plasma so that there are no gaps between the toroidal legs of the coils (i.e., the coils interlock to form a complete shell). In other words,

$$M = \frac{\pi}{\delta\theta}. \tag{62}$$

When these two conditions are satisfied, $Q_0 = 1$, and the present feedback scheme becomes indistinguishable from the idealized scheme discussed in Sec. I. Note that the optimum configuration is to have many, large, overlapping coils.

In reality, of course, it is completely impractical to place a sufficient number of feedback coils around the plasma so that there are no gaps between the toroidal legs of the coils. It is, however, practical to match the poloidal extent of each feedback coil to the poloidal half-wavelength of the central harmonic. Thus in a realistic feedback scheme the optimum value of the critical gain is

$$Q_0 = \frac{\pi}{M\delta\theta} \gg 1. \tag{63}$$

It is clear that, in the absence of coupling to sideband harmonics, a realistic feedback scheme is just as capable of stabilizing the resistive shell mode as the idealized scheme discussed in Sec. I. Admittedly, a realistic feedback scheme is far less efficient than the idealized scheme (i.e., the critical gain is far higher in the former case), but this merely implies that the former scheme requires much more powerful feedback amplifiers than the latter.

D. Approximate solution of the dispersion relation: II

The mode coupling parameter α can be written

$$\alpha \simeq \sum_{j,j\neq 0,m\neq 0}^{m=m_0+jM} \frac{\Delta_w^{m_0}}{\gamma\tau_w + 2|m|} \frac{m_0}{m} \frac{\sin(m\delta\theta/2)\sin^2(m\Delta\theta/2)}{\sin(m_0\delta\theta/2)\sin^2(m_0\Delta\theta/2)}, \tag{64}$$

where use has been made of Eq. (28), which is generally an excellent approximation.[9] In the limit

$$\gamma\tau_w \ll M, \tag{65}$$

the mode coupling parameter becomes independent of the growth rate and reduces to

$$\alpha \simeq \alpha_0 = \frac{\Delta_w^{m_0}}{2m_0} \sum_{j,j\neq 0,m\neq 0}^{m=m_0+jM} \frac{m_0^2}{|m|^2} \frac{\sin(|m|\delta\theta/2)\sin^2(m\Delta\theta/2)}{\sin(m_0\delta\theta/2)\sin^2(m_0\Delta\theta/2)}. \tag{66}$$

In this limit, the feedback modified dispersion relation (57) can be rearranged to give

$$\gamma\tau_w = \Delta_w^{m_0} \frac{1 - \hat{Q}(1-\alpha_0)}{1 + \hat{Q}\alpha_0}. \tag{67}$$

It can be seen, by comparison with the dispersion relation (59), that the main effect of mode coupling is to increase the critical value of the gain beyond which the resistive shell mode is stabilized. In fact, the critical gain becomes

$$Q_c = \frac{Q_0}{1-\alpha_0}. \tag{68}$$

In the absence of mode coupling (i.e., $\alpha_0 = 0$) the critical gain reverts to the value (i.e., $Q_c = Q_0$) obtained in Sec. IV C. Note, however, that if the mode coupling is too strong then the critical gain goes to infinity, and the feedback scheme becomes incapable of stabilizing the resistive shell mode. The critical value of the mode coupling parameter above which the feedback scheme fails is $\alpha_0 = 1$.

It is clear that mode coupling has a highly deleterious effect on feedback stabilization schemes for the resistive shell mode. In fact, if the coupling becomes too strong then a given feedback scheme is incapable of stabilizing the mode, even at very high values of the gain. It follows that, when optimizing the design of the feedback coils for the control of external modes, the principle objective should be to reduce mode coupling (i.e., to make the parameter α_0 as small as practically possible).

The approximate dispersion relation (67) implies that in positive feedback (i.e., when the gain Q is negative) the growth rate of the resistive shell mode becomes infinite when $Q = -Q_0/\alpha_0$. In fact, this is not the case, because the inequality (65), which is used in the derivation of Eq. (67), breaks down when the growth rate becomes large. It is demonstrated in the Appendix that when Q is large and negative the growth rate is finite, positive, and directly proportional to $-Q$.

E. Evaluation of the mode coupling parameter

In the limit

$$M \gg 1, \tag{69}$$

the expression (66) for the mode coupling parameter reduces to

$$\alpha_0 \simeq \frac{\Delta_w^{m_0} m_0}{M^2 \sin(m_0 \delta\theta/2) \sin^2(m_0 \Delta\theta/2)}\, \hat{\alpha}_0(M\delta\theta/2, M\Delta\theta/2), \tag{70}$$

where

$$\hat{\alpha}_0(x,y) = \sum_{j=1}^{\infty} \frac{\sin(jx)\sin^2(jy)}{j^2}. \tag{71}$$

It is easily demonstrated that

$$\hat{\alpha}_0(x,y) = \frac{x}{2}\left[\ln\left(\frac{2|\sin y|}{x}\right) + 1\right] + O(x^3), \tag{72}$$

provided that $|\sin y| \gg x$. For the special case in which $|\sin(M\Delta\theta/2)| \ll M\delta\theta/2$, the expression (66) takes the special value

$$\alpha_0 \simeq \frac{\Delta_w^{m_0} m_0}{M^2 \sin(m_0 \delta\theta/2)}\, \tilde{\alpha}_r(x), \tag{73}$$

where

$$\tilde{\alpha}_0(x) = \sum_{j=1}^{\infty} \frac{\sin(jx)}{j^2} = x\left[\ln\left(\frac{1}{x}\right) + 1\right] + O(x^3). \tag{74}$$

It follows from Eqs. (69)–(74) that, in the limit

$$M \gg 1, \quad M\delta\theta/2 \ll 1, \tag{75}$$

the mode coupling parameter α_0 can be written in the form

$$\alpha_0 \simeq \begin{cases} \dfrac{(m_0/M)}{(r_c/r_w)^{2m_0}-1}\, \dfrac{[\ln(4|\sin(M\Delta\theta/2)|/M\delta\theta)+1]}{\sin^2(m_0\Delta\theta/2)} & \text{for } |l(2\pi/M) - \Delta\theta| \gg \delta\theta \\ \dfrac{2(m_0/M)}{(r_c/r_w)^{2m_0}-1}\, [\ln(2/M\delta\theta)+1] & \text{for } |l(2\pi/M) - \Delta\theta| \ll \delta\theta \end{cases}. \tag{76}$$

Here l is an integer, and use has been made of Eq. (27). Note that the toroidal legs of the feedback loops overlap whenever

$$|l(2\pi/M) - \Delta\theta| < \delta\theta. \tag{77}$$

Thus the upper limit in Eq. (76) corresponds to the case where the toroidal legs of the feedback loops do not overlap, whereas the lower limit corresponds to the case where the toroidal legs of the feedback loops exactly overlay one another. In the latter case, the configuration of feedback loops is best described as an interconnected network of feedback controlled conductors, rather than a set of independent feedback coils.

F. Design of feedback coils: I

Consider the limit $M \gg 1$, discussed in Sec. IV E, in which there are very many feedback coils surrounding the plasma in the poloidal direction. It is possible to identify four different regimes. First, nonoverlapping coils, characterized by

$$M\Delta\theta < 2\pi, \quad m_0\Delta\theta \ll 1. \tag{78}$$

Second, an interconnected network of coils, characterized by

$$M\Delta\theta = 2\pi, \quad m_0\Delta\theta \ll 1. \tag{79}$$

Third, slightly overlapping coils, characterized by

$$M\Delta\theta > 2\pi, \quad m_0\Delta\theta \ll 1, \tag{80}$$

and, fourth, highly overlapping coils, characterized by

$$M\Delta\theta \gg 2\pi, \quad m_0\Delta\theta \sim O(1). \tag{81}$$

The first three regimes are illustrated in Fig. 2.

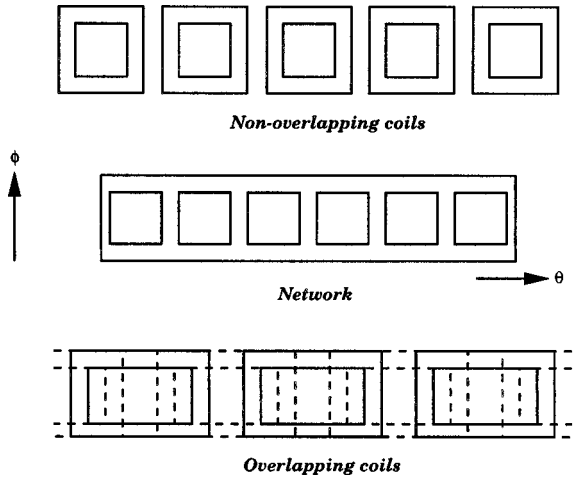

FIG. 2. Three different feedback coil configurations.

Using the results of Sec. IV E, the values of the mode coupling parameter α_0 corresponding to the four different regimes described above are as follows. For both nonoverlapping and slightly overlapping coils,

$$\alpha_0 \simeq \frac{(M/m_0)}{(r_c/r_w)^{2m_0}-1}\,\frac{[\ln(4|\sin(M\Delta\theta/2)|/M\delta\theta)+1]}{(M\Delta\theta/2)^2}. \tag{82}$$

For a network of coils,

$$\alpha_0 \simeq \frac{2(m_0/M)}{(r_c/r_w)^{2m_0}-1}\,[\ln(2/M\delta\theta)+1]. \tag{83}$$

Finally, for highly overlapping coils,

$$\alpha_0 \simeq \frac{(m_0/M)}{(r_c/r_w)^{2m_0}-1}\,\frac{[\ln(4|\sin(M\Delta\theta/2)|/M\delta\theta)+1]}{\sin^2(m_0\Delta\theta/2)}. \tag{84}$$

Recall, from Sec. IV D, that the feedback scheme under investigation in this paper fails completely when the mode coupling parameter α_0 exceeds unity. Thus when comparing two different feedback coil configurations, the configuration which is most effective at stabilizing the resistive shell mode is always the one with the smallest value of the mode coupling parameter α_0 (assuming that the plasma equilibrium and shell radius are the same in both cases).

It is clear from Eq. (82) that both nonoverlapping and slightly overlapping coil configurations possess comparatively large values of the mode coupling parameter α_0. These configurations are, therefore, relatively ineffective at stabilizing the resistive shell mode. Note that $\alpha_0 \propto M$ in Eq. (82), implying that nonoverlapping and slightly overlapping coil configurations become progressively less effective as the number of feedback coils in the poloidal direction is increased. The main reason for the ineffectiveness of these configurations, in the limit $M \gg 1$, is the fact that the poloidal extent of each feedback coil is inevitably much less than the poloidal half-wavelength of the intrinsically unstable m_0,n resistive shell mode.

According to Eq. (83), an interconnected network of feedback coils possesses a comparatively small value of the mode coupling parameter α_0. This configuration is, therefore, fairly effective at stabilizing the resistive shell mode. Note that $\alpha_0 \propto 1/M$ in Eq. (83), implying that a network becomes progressively more effective as the number of feedback coils in the poloidal direction is increased. A comparison of Eqs. (82) and (83) shows that a network is more effective at stabilizing the resistive shell mode than either nonoverlapping or slightly overlapping coil configurations provided that

$$M > 4m_0 \tag{85}$$

(i.e., provided that there are more than four coils per period of the m_0,n mode in the poloidal direction). It follows that the only effective coil configuration in which the poloidal extent of each individual feedback coil is much less than the poloidal half-wavelength of the m_0,n mode is one where neighbouring coils touch, so as to form an interconnected network.

It is clear from Eq. (84) that a highly overlapping coil configuration possesses a particularly small value of the mode coupling parameter α_0. This configuration is, therefore, extremely effective at stabilizing the resistive shell mode. Note that $\alpha_0 \propto 1/M$ in Eq. (84), implying that a highly overlapping coil configuration becomes progressively more effective as the number of feedback coils in the poloidal direction is increased. It follows from Eq. (84) that the most effective coil configuration is one in which the poloidal extent of each feedback coil is equal to the poloidal half-wavelength of the m_0,n mode [see Eq. (61)], and M is not an even multiple of m_0.

G. Numerical results

Strictly speaking, the conclusions of Sec. IV F are only valid in the limit $M \gg 1$, in which there are very many feedback coils surrounding the plasma in the poloidal direction. In order to investigate the more realistic limit in which there are only a few feedback coils surrounding the plasma in the poloidal direction it is necessary to resort to numerical techniques. The results described below were obtained by solving the matrix eigenvalue equation (39) using the $L^{mm'}$ values specified in Eq. (50). The shell stability indices Δ_w^m were calculated using a ''Wesson-like'' plasma current profile,[2]

$$J_\phi(r) = J_\phi(0)\begin{cases}(1-r^2/a^2)^{q_a/q_0-1} & r \leqslant a\\ 0 & r > a,\end{cases} \tag{86}$$

where a is the minor radius of the plasma. The associated safety factor profile takes the form

$$q(r) = q_a\begin{cases}\dfrac{r^2/a^2}{1-(1-r^2/a^2)^{q_a/q_0}} & r \leqslant a\\ r^2/a^2 & r > a\end{cases} \tag{87}$$

Here q_0 and q_a are the values of the safety factor on the magnetic axis and at the plasma boundary, respectively. Sufficient poloidal harmonics were included in the calculation to determine the growth rate of the resistive shell mode to an accuracy of less than 1%. Typically, this required about 160 harmonics.

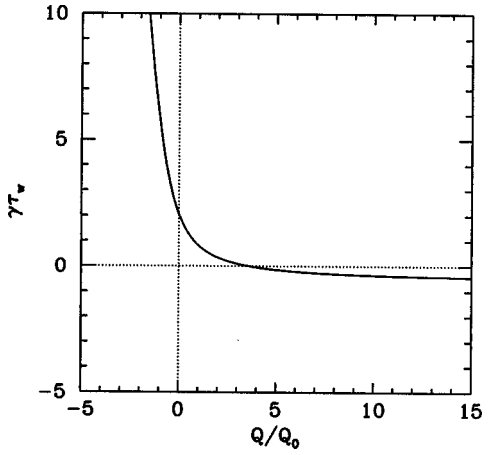

FIG. 3. The feedback modified growth rate γ of the 3,1 resistive shell mode plotted as a function of the gain Q in the feedback circuits. The growth rate is normalized with respect to the time constant τ_w of the shell. The gain is normalized with respect to the critical gain Q_0 needed to stabilize the mode in the absence of coupling to sideband harmonics. The plasma equilibrium is characterized by $q_0=1.3$ and $q_a=2.9$. The critical radius for this equilibrium is $r_c=1.38a$. The radius of the shell is $r_w=1.1a$. The feedback coils are characterized by $M=3$, $\Delta\theta=60°$, and $\delta\theta=10°$.

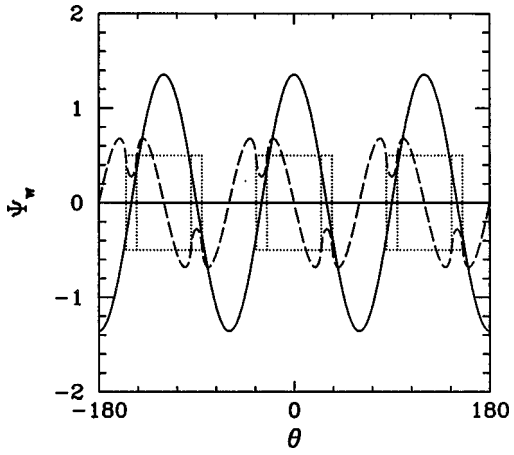

FIG. 4. The shell flux Ψ_w evaluated as a function of the poloidal angle θ for a feedback gain of $Q=3.615Q_0$. The solid and dashed curves show the flux evaluated at two toroidal locations 90° apart (in ϕ). The dotted curves indicate the positions of the feedback coils. The plasma equilibrium is characterized by $q_0=1.3$ and $q_a=2.9$. The central harmonic and critical radius for this equilibrium are 3,1 and $r_c=1.38a$, respectively. The radius of the shell is $r_w=1.1a$. The feedback coils are characterized by $M=3$, $\Delta\theta=60°$, and $\delta\theta=10°$.

Figure 3 shows the feedback modified growth rate of the 3,1 resistive shell mode (normalized with respect to the time constant of the shell) plotted as a function of the gain in the feedback circuits (normalized with respect to the critical gain Q_0 needed to stabilize the resistive shell mode in the absence of coupling to sideband harmonics). The plasma equilibrium is characterized by $q_0=1.3$ and $q_a=2.9$. The critical radius is $r_c=1.38a$ and the radius of the shell is $r_w=1.1a$. The feedback coils are characterized by $M=3$, $\Delta\theta=60°$, and $\delta\theta=10°$. It can be seen that the growth rate versus gain curve exhibits all of the features predicted in Sec. IV D and the Appendix. As the gain is increased from zero, the growth rate is reduced. However, at large positive gains the growth rate asymptotes to a constant value. The critical gain above which the mode is stabilized is larger than the critical gain Q_0 needed to stabilize the mode in the absence of coupling to sideband harmonics. As the gain is decreased below zero, the growth rate increases. At large negative gains the growth rate becomes linearly proportional to $-Q$, and increases very rapidly as Q is decreased. The good agreement between the analytic results of Sec. IV D and the Appendix and the numerical results described above suggest that the qualitative behavior of the feedback scheme is independent of the number of coils in the poloidal direction.

Figure 4 shows the shell flux $\Psi_w(\theta)$ calculated at two toroidal locations 90° apart (in ϕ) for the case in which the feedback gain Q is just large enough to stabilize the mode (i.e., $Q=3.615Q_0$). The other parameters are the same as those used in Fig. 3. The solid curve corresponds to a particular toroidal phase of the 3,1 resistive shell mode at which there is zero flux through the feedback loops, and so no feedback is applied. The dashed curve corresponds to a phase at which flux through the feedback loops attains its maximum value, and so strong feedback is applied. It can be seen that the feedback reduces the mode amplitude, as expected, but also distorts the poloidal structure of the mode, so that the mode is no longer a pure poloidal harmonic. The distortion of the mode, which is achieved via coupling to sideband harmonics, has a deleterious effect on the feedback scheme, since it tends to reduce the ratio of the flux through each feedback loop to the amplitude of the mode; thus effectively reducing the gain in the feedback circuits.

H. Design of feedback coils: II

The analytic results of Sec. IV F can easily be extrapolated to the case where there are only a few coils surrounding the plasma in the poloidal direction. These results predict that when $M\sim O(1)$ the performance of the feedback scheme should improve as $\delta\theta$ increases and r_w/r_c decreases. The analytic results of Sec. IV F also predict that the optimum poloidal angular width of each feedback coil should be half the poloidal wavelength of the intrinsically unstable m_0,n harmonic; i.e., $(\Delta\theta)_{\rm opt}=\pi/m_0$. In the following, these predictions are compared with numerical results.

Figure 5 shows the critical gain Q_c needed to stabilize the 3,1 resistive shell mode plotted as a function of the angular width $\delta\theta$ of the toroidal legs of the feedback coils. Q_c is normalized with respect to the critical gain Q_0 required to stabilize the mode in the absence of sideband coupling. The other parameters are the same as those used in Fig. 3. It can be seen that Q_c decreases as $\delta\theta$ increases. In other words, the performance of the feedback scheme improves as the width of the toroidal legs of the feedback coils increases, which accords well with the predictions of Sec. IV F.

Figure 6 shows the critical gain Q_c needed to stabilize the 3,1 resistive shell mode plotted as a function of the poloidal angular extent $\Delta\theta$ of each feedback coil. Q_c is normalized with respect to the critical gain Q_0 required to stabilize the mode in the absence of sideband coupling. The other parameters are the same as those used in Fig. 3. Data is shown for three values of the edge safety factor: $q_a=2.91$,

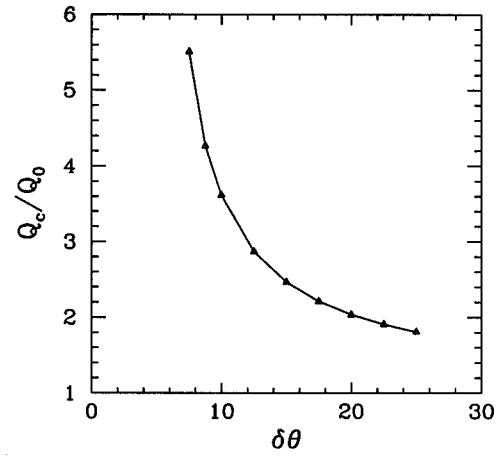

FIG. 5. The critical gain Q_c required to stabilize the 3,1 resistive shell mode plotted as a function of the angular width $\delta\theta$ of the toroidal legs of the feedback coils. The critical gain is normalized with respect to the critical gain Q_0 needed to stabilize the mode in the absence of coupling to sideband harmonics. The plasma equilibrium is characterized by $q_0=1.3$ and $q_a=2.9$. The critical radius and the radius of the shell are $r_c=1.38a$ and $r_w=1.1a$, respectively. The feedback coils are characterized by $M=3$ and $\Delta\theta=60°$.

for which the mode is moderately unstable; $q_a=2.85$, for which the mode is only slightly unstable; and $q_a=2.90$, which is an intermediate case. It can be seen that when the mode is only slightly unstable there is a wide range of values of $\Delta\theta$ for which the performance of the feedback scheme is close to optimal (i.e., $Q_c\simeq Q_0$). However, the performance degrades rapidly as the mode becomes more unstable. This degradation proceeds most slowly when $\Delta\theta\simeq 60°$; i.e., when the poloidal width of the feedback coils is close to the analytically predicted optimal value, $\pi/m_0=60°$. When the mode becomes sufficiently unstable the feedback scheme fails completely unless $\Delta\theta$ lies very close to the optimal value. However, even in this case, the critical gain needed to stabilize the mode is strongly increased by mode coupling. Note that when there are only a few coils surrounding the plasma in the poloidal direction the optimum configuration is for the coils to be nonoverlapping. Overlapping coils only become the optimum configuration when

$$M>2m_0. \tag{88}$$

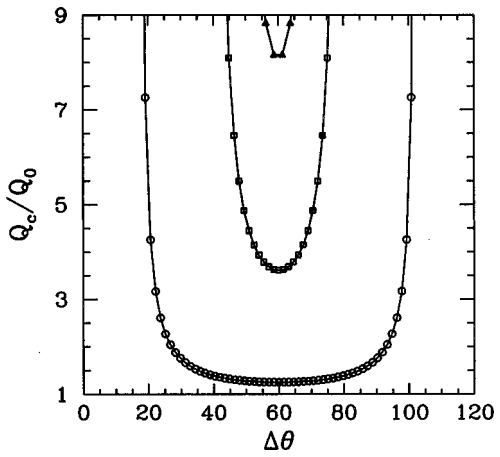

FIG. 6. The critical gain Q_c required to stabilize the 3,1 resistive shell mode plotted as a function of the poloidal angular extent $\Delta\theta$ of each feedback coil. The critical gain is normalized with respect to the critical gain Q_0 needed to stabilize the mode in the absence of coupling to sideband harmonics. The triangular, square, and circular data points correspond to $q_a=2.91$, 2.90, and 2.85, respectively. The corresponding values of the critical radius are $r_c=1.35$, 1.38, and 1.65, respectively. The plasma equilibrium is characterized by $q_0=1.3$. The radius of the shell is $r_w=1.1a$. The feedback coils are characterized by $M=3$ and $\delta\theta=10°$.

I. Design of feedback coils: III

The results of Sec. IV H were obtained by solving the matrix eigenvalue equation (39) and then searching for the critical value of the feedback gain, Q_c, at which the growth rate γ of the resistive shell mode becomes zero. There is, however, a far simpler, but slightly less accurate, method of calculating Q_c. Note, from Eq. (68), that Q_c/Q_0 is completely determined by the mode coupling parameter α_0. This parameter is easily evaluated by summing the series (66). In fact,

$$\alpha_0\simeq\frac{\sigma_0}{(r_c/r_w)^{2m_0}-1}, \tag{89}$$

where

$$\sigma_0=\sum_{j,j\neq 0,m\neq 0}^{m=m_0+jM}\frac{m_0^2}{m^2}\frac{\sin(|m|\,\delta\theta/2)\sin^2(m\Delta\theta/2)}{\sin(m_0\delta\theta/2)\sin^2(m_0\Delta\theta/2)}. \tag{90}$$

Here use has been made of Eq. (27). The feedback scheme is incapable of stabilizing the resistive shell mode when

$$\alpha_0\geqslant 1. \tag{91}$$

This corresponds to

$$r_c\leqslant r_e, \tag{92}$$

where

$$r_e=r_w(1+\sigma_0)^{1/2m_0}. \tag{93}$$

Thus in the limit in which the gain Q is large and positive, the plasma is stable when $r_c<r_e$ and unstable when $r_c\geqslant r_e$. In other words, the feedback modified stability boundaries of the plasma are the same as those of a plasma surrounded by a perfectly conducting shell of radius r_e. The quantity r_e is termed the ''equivalent radius'' of the feedback modified resistive shell. Obviously, in order for the shell to be effective at stabilizing external modes it must have a relatively small equivalent radius. Thus a given feedback scheme can be optimized by minimizing r_e subject to practical constraints. The critical gain Q_c needed to stabilize the resistive shell mode is related to the equivalent radius via

$$\frac{Q_c}{Q_0}=\frac{(r_c)^{2m_0}-(r_w)^{2m_0}}{(r_c)^{2m_0}-(r_e)^{2m_0}}, \tag{94}$$

assuming that

$$r_e>r_c>r_w. \tag{95}$$

Note that when $r_c>r_e$ the feedback scheme is incapable of stabilizing the resistive shell mode. On the other hand, when

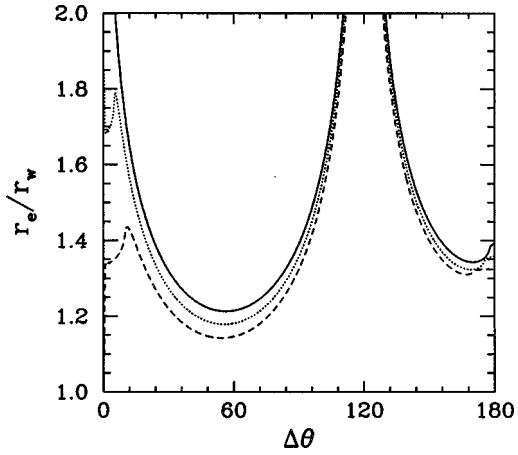

FIG. 7. The equivalent radius r_e plotted as a function of the poloidal angular extent $\Delta\theta$ of each feedback coil. The equivalent radius is normalized with respect to the radius r_w of the shell. The solid, dotted, and dashed curves correspond to $\delta\theta=5°$, 10°, and 20°, respectively. The central harmonic is $m_0,n=3,1$. The feedback coils are characterized by $M=4$.

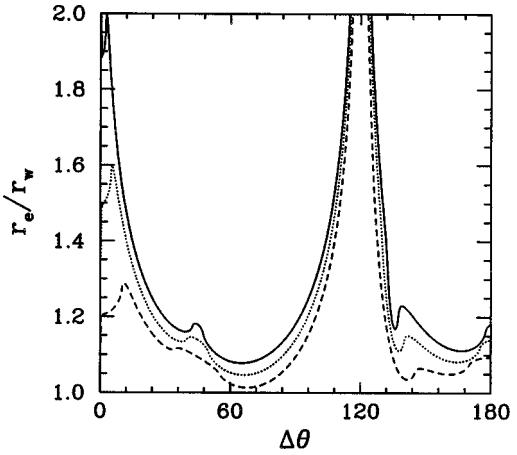

FIG. 8. The equivalent radius r_e plotted as a function of the poloidal angular extent $\Delta\theta$ of each feedback coil. The equivalent radius is normalized with respect to the radius r_w of the shell. The solid, dotted, and dashed curves correspond to $\delta\theta=5°$, 10°, and 20°, respectively. The central harmonic is $m_0,n=3,1$. The feedback coils are characterized by $M=8$.

$r_w>r_c$ the resistive shell mode is intrinsically stable, and so there is no need to switch the feedback system on.

Figure 7 shows the equivalent radius r_e, evaluated from Eqs. (90) and (93), plotted as a function of the poloidal angular extent $\Delta\theta$ of each feedback coil for a case in which there are four evenly spaced feedback coils in the poloidal direction, and the poloidal mode number of the intrinsically unstable harmonic is $m_0=3$. The equivalent radius is normalized with respect to the radius r_w of the resistive shell. Note from Eqs. (90) and (93) that

$$r_e(\Delta\theta+k\pi)=r_e(\Delta\theta), \tag{96}$$

where k is an integer, so it is only necessary to calculate r_e for $\Delta\theta$ in the range 0°–180°. Broadly speaking, it can be seen that the equivalent radius r_e tends to infinity (i.e., the feedback scheme becomes completely ineffective) whenever the poloidal extent of each feedback coil is equal to an integer multiple of the poloidal wavelength of the intrinsically unstable harmonic; i.e., whenever

$$\Delta\theta=k\,\frac{2\pi}{m_0}, \tag{97}$$

where k is a non-negative integer. On the other hand, the equivalent radius attains a minimum value (i.e., the feedback scheme is optimized) whenever the poloidal extent of each feedback coil is equal to a half-integer multiple of the poloidal wavelength of the intrinsically unstable harmonic; i.e., whenever

$$\Delta\theta=(2k+1)\,\frac{\pi}{m_0}, \tag{98}$$

where k is a non-negative integer. The smallest area feedback coils which give optimal performance are such that the poloidal extent of each coil is equal to half the wavelength of the intrinsically unstable harmonic; i.e., $\Delta\theta=\pi/m_0=60°$ (see Sec. IV H). Note that in this configuration the coils do not overlap [see Eq. (88)]. It is clear from Fig. 7 that the equivalent radius r_e is far less sensitive to variations in the angular thickness $\delta\theta$ of the toroidal legs of the feedback coils than to variations in $\Delta\theta$. Note that r_e decreases as $\delta\theta$ increases (see Sec. IV H). According to Fig. 7, when properly optimized, a feedback scheme employing four evenly spaced coils in the poloidal direction can make a resistive shell interacting with a 3,1 external mode act like a perfectly conducting shell whose radius is approximately 20% larger than that of the resistive shell. The strong variation of r_e with $\Delta\theta$ exhibited in Fig. 7 suggests that a feedback scheme which employs a small number of coils in the poloidal direction can only be optimized for one particular poloidal mode number (i.e., a scheme optimized for $m_0=3$ modes is unlikely to work effectively for $m_0=2$ or $m_0=3$ modes).

Figure 8 shows the equivalent radius r_e, evaluated from Eqs. (90) and (93), plotted as a function of the poloidal angular extent $\Delta\theta$ of each feedback coil for a case in which there are eight evenly spaced feedback coils in the poloidal direction, and the poloidal mode number of the intrinsically unstable harmonic is $m_0=3$. The equivalent radius is normalized with respect to the radius r_w of the resistive shell. The variation of r_e with $\Delta\theta$ is broadly similar to that exhibited in Fig. 7. The ''features'' in the r_e versus $\Delta\theta$ curves at $\Delta\theta=45°$ and 135°, which are evident in Fig. 8, correspond to the cases where the (toroidal legs of the) feedback coils touch so as to form a single layer network and a triple layer network, respectively. In general, the coils touch so as to form an l-layer network whenever

$$\Delta\theta=l\,\frac{2\pi}{M}. \tag{99}$$

According to Eqs. (76), (89), and (93), an l-layer network has a smaller equivalent radius than similar coil configurations in which the coils do not touch if

$$2\sin^2(l\pi m_0/M)<1. \tag{100}$$

Likewise, an l-layer network has a larger equivalent radius than similar coil configurations in which the coils do not touch if

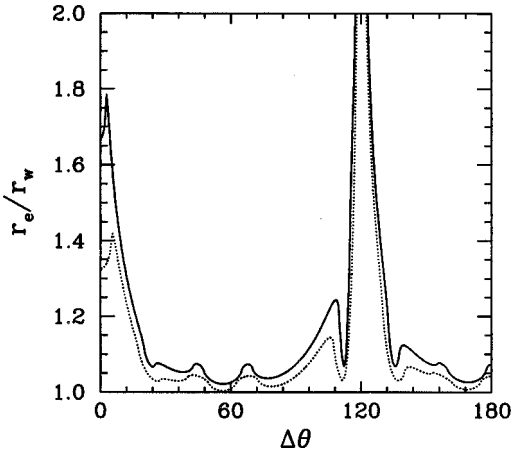

FIG. 9. The equivalent radius r_e plotted as a function of the poloidal angular extent $\Delta\theta$ of the feedback coils. The equivalent radius is normalized with respect to the radius r_w of the shell. The solid and dotted curves correspond to $\delta\theta=5°$ and 10°, respectively. The central harmonic is $m_0,n=3,1$. The feedback coils are characterized by $M=16$.

$$2\sin^2(l\pi m_0/M)>1. \tag{101}$$

According to Eqs. (100) and (101), a single layer network ($\Delta\theta=45°$) should have a larger equivalent radius than nontouching coil configurations with similar values of $\Delta\theta$, a double layer network ($\Delta\theta=90°$) should have exactly the same equivalent radius as nontouching coil configurations with similar values of $\Delta\theta$, and a triple layer network ($\Delta\theta=135°$) should have a smaller equivalent radius than nontouching coil configurations with similar values of $\Delta\theta$. Furthermore, according to Eqs. (76), (89), and (93), all networks should have the same equivalent radius, irrespective of the number of layers which they contain. It can be seen that all of these predictions are borne out in Fig. 8. Note that the feature at $\Delta\theta=45°$ has the effect of displacing the optimum value of $\Delta\theta$ (i.e., the value at which r_e is minimized) so that it becomes slightly larger than 60°. The optimum configuration consists of overlapping coils [see Eq. (88)].

Figure 9 shows the equivalent radius r_e, evaluated from Eqs. (90) and (93), plotted as a function of the poloidal angular extent $\Delta\theta$ of each feedback coil for a case in which there are sixteen evenly spaced feedback coils in the poloidal direction, and the poloidal mode number of the intrinsically unstable harmonic is $m_0=3$. The equivalent radius is normalized with respect to the radius r_w of the resistive shell. Features are evident in the r_e versus $\Delta\theta$ curves at $\Delta\theta=22.5°$, 45°, 67.5°, 112.5°, 135°, and 157.5°, respectively. These features correspond to cases where (the toroidal legs of) the feedback coils touch so as to form networks [see Eq. (99)]. Note that, as expected, the value of r_e is approximately the same for each network. The many features have the effect of flattening the r_e versus $\Delta\theta$ curves, so that r_e/r_w is more or less constant, and fairly close to unity, over a wide range of values of $\Delta\theta$. In fact, the only values of $\Delta\theta$ for which r_e/r_w becomes much larger than unity correspond either to the case where the poloidal angular extent of each feedback coil is close to an integer multiple of the poloidal wavelength of the intrinsically unstable harmonic, or to the case where the poloidal extent of each feedback coil becomes sufficiently small that the coils do not overlap (see Sec. IV F). It is clear that a feedback scheme which employs a large number of overlapping feedback coils in the poloidal direction can easily be optimized so that it works effectively for a range of poloidal mode numbers (i.e., a scheme optimized for $m_0=3$ modes is also likely to work effectively for $m_0=2$ and $m_0=4$ modes).

V. NON-EVENLY SPACED COILS

A. Introduction

Suppose that the feedback coils are not evenly spaced in the poloidal direction. In practice, this is often the case because, for engineering reasons, it is difficult to install feedback coils on the inboard side of a toroidal device. Thus in most tokamaks the feedback coils are all located on the outboard side of the device. This section describes how the analysis of Sec. IV can be modified and extended to deal with non-evenly spaced feedback coils.

B. Two coils

The simplest nontrivial example of non-evenly spaced feedback coils is that where there are two coils which are not diagrammatically opposite one another in the poloidal plane. This case corresponds to $M=2$, $\theta_1=+\theta_*/2$, and $\theta_2=-\theta_*/2$ (where $\theta_*\neq 180°$), in the notation of Sec. III. The elements of the **B** matrix [see Eq. (47)] can be written

$$B_{11}=B_{22}=\frac{\hat{Q}}{2}\,(g-b_{11}), \tag{102a}$$

$$B_{12}=B_{21}^*=\frac{\hat{Q}}{2}\,(g-b_{12}), \tag{102b}$$

where

$$g=\frac{\Delta_w^{m_0}}{\Delta_w^{m_0}-\gamma\tau_w}, \tag{103}$$

and

$$b_{11}=\sum_m^{m\neq 0,m\neq m_0}\frac{\Delta_w^{m_0}}{\gamma\tau_w-\Delta_w^m}\,\frac{m_0}{m}\,\frac{\sin(m\delta\theta/2)\sin^2(m\Delta\theta/2)}{\sin(m_0\delta\theta/2)\sin^2(m_0\Delta\theta/2)}, \tag{104a}$$

$$b_{12}=\sum_m^{m\neq 0,m\neq m_0}\frac{\Delta_w^{m_0}}{\gamma\tau_w-\Delta_w^m}\,\frac{m_0}{m}\,\frac{\sin(m\delta\theta/2)\sin^2(m\Delta\theta/2)}{\sin(m_0\delta\theta/2)\sin^2(m_0\Delta\theta/2)}\times e^{i(m-m_0)\theta_*}. \tag{104b}$$

The feedback modified dispersion relation for the resistive shell mode is obtained from the solubility condition for Eq. (44) [i.e., $\det(\mathbf{A})=0$],

$$[1-\hat{Q}(g-b_{11})/2]^2-\hat{Q}^2(g-b_{12})(g-b_{12}^*)/4=0. \tag{105}$$

This expression can be rearranged to give

$$\gamma\tau_w=\Delta_w^{m_0}\frac{1-\hat{Q}(1-b_{11})+\hat{Q}^2[b_{11}^2-|b_{12}|^2-2b_{11}+2\,\mathrm{Re}(b_{12})]/4}{1+\hat{Q}b_{11}+\hat{Q}^2(b_{11}^2+|b_{12}|^2)/4}. \tag{106}$$

There are two regimes of interest. For $\alpha_0<1$, where

$$\alpha_0=\frac{1}{2}\frac{\overline{b}_{11}^2-|\overline{b}_{12}|^2}{\overline{b}_{11}-\mathrm{Re}(\overline{b}_{12})}, \tag{107}$$

the resistive shell mode is unstable for Q in the range $0<Q<Q_c$, where

$$Q_c=\frac{2Q_0}{1-\overline{b}_{11}+|1-\overline{b}_{12}|}, \tag{108}$$

and is stable for $Q\geqslant Q_c$. For $\alpha_0\geqslant 1$, the resistive shell mode is unstable for all positive values of the gain, Q. Here

$$\overline{b}_{ij}=\lim_{\gamma\to 0} b_{ij}. \tag{109}$$

It can be seen that the parameter α_0, defined in Eq. (107), plays an analogous role to the mode coupling parameter α_0 defined in Sec. IV. In particular, the feedback scheme is only capable of stabilizing the resistive shell mode provided that $\alpha_0<1$.

An alternative and far simpler method of determining the form of the generalized mode coupling parameter α_0 is described below. In the limit $\hat{Q}\to\infty$ and $\gamma\to 0$, the solubility condition for Eq. (44) [i.e., $\det(\mathbf{A})=0$] reduces to

$$\begin{vmatrix} g-\overline{b}_{11} & g-\overline{b}_{12}\\ g-\overline{b}_{12}^{*} & g-\overline{b}_{11}\end{vmatrix}=0. \tag{110}$$

The root $g=g_0$ of this equation (which is linear in g) is given by

$$g_0=\frac{1}{2}\frac{\overline{b}_{11}^2-|\overline{b}_{12}|^2}{\overline{b}_{11}-\mathrm{Re}(\overline{b}_{12})}. \tag{111}$$

It is clear from Eq. (103) that if $g_0<1$ then $\gamma<0$ in the limit $\hat{Q}\to\infty$. On the other hand, if $g_0\geqslant 1$ then $\gamma\geqslant 0$ in the limit $\hat{Q}\to\infty$. It follows that only $g_0<1$ is consistent with the successful feedback stabilization of the resistive shell mode. Thus the generalized mode coupling parameter α_0 can be identified with the root g_0 of Eq. (110). It follows that α_0 is simply the root of

$$\begin{vmatrix} \alpha_0-\overline{b}_{11} & \alpha_0-\overline{b}_{12}\\ \alpha_0-\overline{b}_{12}^{*} & \alpha_0-\overline{b}_{11}\end{vmatrix}=0. \tag{112}$$

C. General solution

Suppose that there are M feedback coils in the poloidal direction, with the kth coil centered on poloidal angle θ_k, where k runs from 1 to M. By analogy with Eq. (112), the generalized mode coupling parameter α_0 is the root of

$$|\alpha_0\mathbf{1}-\mathbf{P}|=0, \tag{113}$$

where

$$P_{jk}=\frac{R_{jk}}{(r_c/r_w)^{2m_0}-1}, \tag{114}$$

and

$$R_{jk}=\sum_{m}^{m\neq 0,m\neq m_0}\frac{m_0^2}{m^2}\frac{\sin(|m|\delta\theta/2)\sin^2(m\Delta\theta/2)}{\sin(m_0\delta\theta/2)\sin^2(m_0\Delta\theta/2)}\times e^{i(m-m_0)(\theta_j-\theta_k)}. \tag{115}$$

Here use has been made of Eqs. (27), (28), (104), and (109). Note that Eq. (113) is linear in α_0, so this equation possesses a single root. As before, the feedback scheme is only capable of stabilizing the resistive shell mode provided that $\alpha_0<1$. Thus the optimization procedure is to minimize α_0 subject to practical constraints.

By analogy with Sec. IV I, a feedback modified resistive shell of radius r_w has the same effect on the stability of external modes as an ideal shell of radius r_e. The equivalent radius r_e is given by

$$r_e=r_w(1+\sigma_0)^{1/2m_0}, \tag{116}$$

where $\sigma_0=[(r_c/r_w)^{2m_0}-1]\alpha_0$. The parameter σ_0 can be obtained, more directly, as the root of

$$|\sigma_0\mathbf{1}-\mathbf{R}|=0, \tag{117}$$

where the elements of the $\mathbf{R}$ matrix are specified in Eq. (115). Thus an alternative optimization procedure is to minimize r_e subject to practical constraints.

D. Numerical results

The following results were obtained by solving Eqs. (116) and (117) for the case where the feedback coils do not cover the whole surface of the plasma. To be more exact, if there are M coils in the poloidal direction (where $M>1$), then the coils are centered on the poloidal angles

$$\theta_k=f\left(1-\frac{1}{M}\right)\left(\frac{k-1}{M-1}-\frac{1}{2}\right), \tag{118}$$

for $k=1$ to M, where f is the fraction of the plasma surface covered by coils. It is easily demonstrated that when $f=1$ (i.e., when the whole surface of the plasma is covered by coils), Eqs. (116) and (117) yield the same value for the effective radius r_e as Eqs. (90) and (93).

Figure 10 shows the equivalent radius r_e, evaluated from Eqs. (116) and (117), plotted as a function of the poloidal angular extent $\Delta\theta$ of each feedback coil for a case in which there are five coils in the poloidal direction which do not necessarily cover the whole surface of the plasma. The poloidal mode number of the intrinsically unstable harmonic is $m_0=3$. The equivalent radius is normalized with respect to the radius r_w of the resistive shell. When the coils completely cover the surface of the plasma (i.e., when $f=1$) the optimum configuration is for $\Delta\theta$ to be about 50°, which cor-

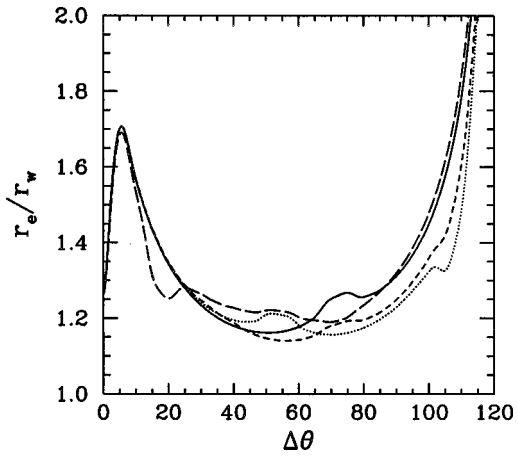

FIG. 10. The equivalent radius r_e plotted as a function of the poloidal angular extent $\Delta\theta$ of the feedback coils. The equivalent radius is normalized with respect to the radius r_w of the shell. The solid, dotted, short-dashed, and long-dashed curves correspond to $f=1$, 0.75, 0.5, and 0.25, respectively, where f is the fraction of the plasma surface covered by feedback coils. The central harmonic is $m_0, n=3,1$. The feedback coils are characterized by $M=5$ and $\delta\theta=10°$.

responds to nonoverlapping coils. As the fraction of the plasma surface covered by the coils is gradually decreased, the performance of the optimum coil configuration initially improves (i.e., r_e decreases). For instance, when the coils only cover half the surface of the plasma (i.e., when $f=0.5$) the optimum configuration is for $\Delta\theta$ to be about 60°, which corresponds to overlapping coils, and the corresponding value of r_e is significantly less than that for the case where the coils cover the whole surface of the plasma. Note, however, that if the fraction of the plasma surface covered by the coils becomes too small (i.e., $f\leqslant 0.25$) then the performance of the optimum coil configuration rapidly worsens (i.e., r_e increases) as f decreases.

The above results suggest that when there are only a few feedback coils in the poloidal direction, so that the optimum configuration when the coils cover the whole surface of the plasma is for the coils to be nonoverlapping, it is advantageous to reconfigure the coils so that they do not cover the whole surface of the plasma, as long as the coils overlap in the new configuration. In other words, the advantages of having overlapping coils can offset the disadvantages of having a set of coils which does not cover the whole surface of the plasma. Of course, this process can only be taken so far: it is never advantageous to have a set of coils which only covers a tiny fraction of the plasma surface. It is easily demonstrated that when there are many feedback coils in the poloidal direction, so that the optimum configuration when the coils cover the whole surface of the plasma is for the coils to overlap, it is never advantageous to reconfigure the coils so that they do not cover the whole surface of the plasma.

VI. SUMMARY AND CONCLUSIONS

The main aim of this paper is to develop a formalism for optimizing the design of feedback coils placed around a tokamak plasma in order to control the resistive shell mode. To achieve this goal it is first necessary to understand the mechanisms by which feedback schemes for stabilizing the resistive shell mode fail to operate effectively. It is demonstrated, in this paper, that the principle failure mechanism is the distortion of the mode structure by the currents circulating around the feedback coils. If this distortion becomes sufficiently strong, it causes the mode to escape through the gaps between the coils, or through the centers of the coils. The principle goal of the optimization process is to reduce mode distortion by minimizing the coupling of different cylindrical Fourier harmonics due to the currents circulating around the feedback coils. It is possible to define a quantity α_0 which parametrizes the strength of the coupling between different Fourier harmonics due to the feedback currents. Feedback fails for $\alpha_0\geqslant 1$. The optimum configuration of the feedback coils is simply that which minimizes α_0, subject to certain practical constraints (e.g., only a fixed number of feedback coils, or only a certain fraction of the plasma surface covered by coils).

For the case in which there are very many evenly spaced feedback coils surrounding the plasma in the poloidal direction, it is possible to derive an analytic expression for the mode coupling parameter α_0 [see Eq. (76)]. Thus in this case, the optimization process can be performed analytically (see Sec. IV F). For the case in which there are only a few evenly spaced feedback coils surrounding the plasma in the poloidal direction, the mode coupling parameter α_0 is obtained by performing a simple summation [see Eqs. (89) and (90)]. Clearly, in this case, the optimization process must be performed numerically [see Sec. IV I]. Finally, for the case in which the feedback coils are not evenly spaced in the poloidal direction, the mode coupling parameter α_0 is obtained by setting the determinant of some matrix equal to zero [see Eq. (113)]. Each element of the matrix is calculated by performing a simple summation [see Eqs. (114) and (115)]. Thus in this case, the optimization must also be performed numerically (see Sec. V D).

The optimal configuration is for the poloidal angular extent of each feedback coil to equal approximately half the poloidal wavelength of the resistive shell mode (see Figs. 6–10). This inevitably leads to the overlapping of neighboring coils when there are many coils surrounding the plasma in the poloidal direction. In fact, the only effective coil configuration in which the poloidal extent of each feedback coil is much less than the poloidal half-wavelength of the resistive shell mode is one where neighboring coils touch, so as to form an interconnected network of feedback controlled conductors surrounding the plasma (see Sec. IV F). When there are only a few coils surrounding the plasma in the poloidal direction, the optimal configuration is not for the set of coils to cover the whole surface of the plasma, since this forces the coils to be nonoverlapping. Instead, the optimum configuration is for the coils to overlap, but only partially cover the surface of the plasma (see Sec. V D). On the other hand, when there are many coils surrounding the plasma in the poloidal direction, the optimum configuration is always for the set of coils to cover the whole surface of the plasma (see Sec. V). A feedback scheme which employs a small number of coils in the poloidal direction can only be optimized for one particular poloidal mode number (see Sec.

IV I). On the other hand, a feedback scheme which employs a large number of overlapping feedback coils in the poloidal direction can easily be optimized so that it works effectively for a range of poloidal mode numbers (see Sec. IV I).

It is always possible to convert the mode coupling parameter α_0 into the equivalent radius r_e of an ideal shell which has the same stabilizing effect on external modes as the feedback modified resistive shell [see Eqs. (89) and (93)]. Thus an alternative optimization procedure is to minimize r_e subject to practical constraints.

Some of the above results (in particular, the result that the optimal poloidal angular extent of each feedback coil is approximately half the poloidal wavelength of the resistive shell mode) are similar to those obtained in an earlier study[11] which deals with a fundamentally different type of feedback algorithm to that employed in this paper. This suggests that the optimal feedback coil configuration for stabilizing the resistive shell mode may be a property of the mode, rather than the feedback algorithm. In other words, the optimization method outlined above may well be independent of the details of the feedback algorithm.

Toroidal effects are completely ignored in this paper. The only justification for this rather drastic approximation is the complexity and novelty of the cylindrical results. The additional effects introduced into the feedback problem by toroidicity in a high-β tokamak include the increased efficiency of feedback coils located on the outboard side of the device compared to those located on the inboard side,[12] as well as the well-known toroidicity and pressure-induced coupling of different poloidal harmonics (which occurs in addition to the coupling induced by the feedback coils). In general, the full toroidal problem can only be investigated via complex and expensive computer simulations.[12] It is hoped that the relatively simple analysis outlined in this paper can be used to greatly narrow the range of parameter space which needs to be investigated in detail using such simulations.

ACKNOWLEDGMENTS

Much of the research reported in this paper was performed while the author was visiting the Department of Applied Physics of Columbia University during the summer of 1997. The author gratefully acknowledges Professor M. E. Mauel and Professor G. A. Navratil for making this visit possible.

This research was funded by the U.S. Department of Energy under Contract No. DE-FG05-96ER-54346.

APPENDIX: POSITIVE FEEDBACK

Consider the analysis of Sec. IV. Suppose that the gain Q in the feedback circuits is large and negative, so that the m_0,n resistive shell mode is subject to strong positive feedback, and its growth rate, consequently, becomes very large. In the limit

$$\gamma\tau_w \gg M \tag{A1}$$

the mode coupling parameter α reduces to [see Eq. (64)]

$$\alpha \simeq \frac{\Delta_w^{m_0}}{\gamma\tau_w}\,\alpha_\infty, \tag{A2}$$

where

$$\alpha_\infty = \sum_{j,j\neq 0,m\neq 0}^{m=m_0+jM} \frac{m_0}{m}\,\frac{\sin(m\,\delta\theta/2)\sin^2(m\Delta\theta/2)}{\sin(m_0\delta\theta/2)\sin^2(m_0\Delta\theta/2)}. \tag{A3}$$

In this limit, the feedback modified dispersion relation (57) can be rearranged to give

$$\gamma\tau_w = \Delta_w^{m_0}(-\hat{Q})(1+\alpha_\infty). \tag{A4}$$

Thus when the gain Q is sufficiently large and negative, the growth rate of the m_0,n resistive shell mode becomes directly proportional to $-Q$.

In the limit

$$M \gg 1 \tag{A5}$$

the expression (A3) for the parameter α_∞ yields

$$\alpha_\infty \simeq \begin{cases} \dfrac{1}{2\sin^2(m_0\Delta\theta/2)}\left(\dfrac{2\pi}{M\,\delta\theta}-1\right) & \text{for } |l(2\pi/M)-\Delta\theta| \gg \delta\theta \\ \left(\dfrac{2\pi}{M\,\delta\theta}-1\right) & \text{for } |l(2\pi/M)-\Delta\theta| \ll \delta\theta \end{cases}. \tag{A6}$$

Here l is an integer. Note that $\alpha_\infty \gg 1$ for a realistic set of feedback coils (i.e., one with $\delta\theta \ll 2\pi/M$).

[1]The conventional definition of this parameter is $\beta = 2\mu_0\langle p\rangle/\langle B^2\rangle$, where $\langle\cdots\rangle$ denotes a volume average, p is the plasma pressure, and B is the magnetic field strength.
[2]J. A. Wesson, Nucl. Fusion **18**, 87 (1978).
[3]J. P. Goedbloed, D. Pfirsch, and H. Tasso, Nucl. Fusion **12**, 649 (1972).
[4]A. Bondeson and D. J. Ward, Phys. Rev. Lett. **72**, 2709 (1994).
[5]R. Betti and J. P. Freidberg, Phys. Rev. Lett. **74**, 2949 (1995).
[6]R. Fitzpatrick and A. Y. Aydemir, Nucl. Fusion **36**, 11 (1996).
[7]The standard large aspect-ratio, low-β tokamak ordering is $R_0/a \gg 1$ and $\beta \sim (a/R_0)^2$, where R_0 and a are the major and minor radii of the plasma, respectively.
[8]R. Fitzpatrick, Nucl. Fusion **33**, 1049 (1993).
[9]R. Fitzpatrick, Phys. Plasmas **1**, 2931 (1994).
[10]T. H. Jensen and R. Fitzpatrick, Phys. Plasmas **4**, 2997 (1997).
[11]R. Fitzpatrick, Phys. Plasmas **4**, 4043 (1997).
[12]D. J. Ward, Phys. Plasmas **3**, 3653 (1996).